Fourteenth USA/Europe Air Traffic Management Research and Development Seminar (ATM2021)

Data-Driven Analysis Method for Calculated Time Over in Air Traffic Flow Management

Estimating Achievable Airborne Delay and Acceptance Rate of Calculated Time Over

Daichi Toratani, Yoichi Nakamura, and Megumi Oka
Air Traffic Management department
Electronic Navigation Research Institute (ENRI)
Tokyo, Japan
toratani-d@mpat.go.jp, y-nakamura@mpat.go.jp, kuri@mpat.go.jp

***Abstract*—Due to limited airspace and airport capacity, excessive traffic demand overwhelms air traffic control and causes traffic delays. Air traffic flow management (ATFM) is widely used to prevent excessive traffic demand. ATFM regulates air traffic using traffic management initiatives (TMIs), such as ground delay, miles-in-trail, and speed adjustment. In Japan, the Calculated Fix Departure Time (CFDT), also known as the Calculated Time Over, is being developed as an additional TMI, and trials on CFDT operation have been conducted. The CFDT can be performed if pilots accept the CFDT assigned by the ATFM system. Therefore, a CFDT procedure with a high acceptance rate by pilots is necessary to establish effective CFDT operation. To estimate the acceptance rate, this study develops an analysis method for CFDT operation using data collected in trial operations. With the estimated acceptance rate, the potential performance of the CFDT operation can be quantitatively discussed. The proposed analysis method can contribute to the design of an efficient procedure for CFDT operation by providing the estimated acceptance rate.**

***Keywords*—air traffic flow management (ATFM); traffic management initiatives (TMIs); calculated time over (CTO); speed control**

I. Introduction

Due to the limited capacity of air traffic control, such as the processing capacity of the air traffic controller (ATCo) and the runway capacity, the traffic demand should not exceed the capacity of the airspace and airport. If the traffic demand exceeds the capacity, the ATCo instructs aircraft to delay their arrival using vectoring or airborne holding. However, excessive vectoring and airborne holding cause the aircraft to burn more fuel; therefore, the air traffic flow should be regulated in the presence of excess demand. To prevent excess demand, air traffic flow management (ATFM) is widely used [1]. ATFM regulates the air traffic flow using various techniques, such as ground delay/stop, minutes/miles-in-trail, speed adjustment, and rerouting. These techniques are called traffic management initiatives (TMIs) [2].

In addition to the above TMIs, the Japan Civil Aviation Bureau employs the Calculated Fix Departure Time (CFDT), also known as the Calculated Time Over [3]. The CFDT is a TMI that assigns a time to fly over a specific waypoint for in-flight aircraft. A similar concept, Long-Range ATFM, has been developed in New Zealand and Singapore [4]. The ground delay, which assigns the Expected Departure Clearance Time to departing aircraft, is also a time-assignment TMI. However, the ground delay can only be assigned to flights departing from domestic airports. Accordingly, using only the ground delay, only domestic flights are delayed to prevent excess demand, which leads to unfairness between domestic and inbound flights. In contrast, the CFDT can be assigned to both domestic and inbound flights; therefore, the CFDT has the potential to improve the fairness of ATFM. Additionally, the CFDT can serve as an initial step to achieve trajectory-based operations.

An operational trial of the CFDT began in 2011 [5] but was interrupted in 2014 due to technical reasons, including inconsistency of the trajectory estimation between onboard and ground systems. With improvements in the operational procedure and ground systems, the CFDT trial will resume. A trial called Shadow Operation beginning in 2020 is currently underway. In this trial, the CFDT is not instructed to the pilot, and the aircraft does not change the cruise speed. Instead, fundamental data regarding the CFDT operation are collected, such as the estimated time of arrival (ETA) at a specific waypoint derived by onboard and ground systems. Through analysis of the data collected in the Shadow Operation, the CFDT will resume in actual operation.

This paper investigates an analysis method for CFDT operation. One important factor for CFDT operation is the acceptance rate, which is the rate at which an assigned CFDT is accepted by a pilot. The method for estimating the acceptance rate is developed using the data collected in the operational trials. By analyzing the acceptance rate, this study can contribute to establishing the best means of implementing CFDT operation. The remainder of this paper is structured as follows. Section II summarizes CFDT operation, including the concept, operational environment, problem, and operational model. Sections III and IV describe the trial operation from 2011 to 2014 and Shadow Operation, respectively. These sections also describe the data collected in each trial and the method of analyzing the collected data.

Section V discusses the use of the proposed analysis method and ways to contribute to the design of CFDT operation. Section VI concludes the paper.

II. Calculated Fix Departure Time

A. Concept of CFDT

Fig. 1 presents the procedure of the CFDT operation. Here, "CFDT" refers to the time at which the aircraft must fly over the fix, while "CFDT fix" refers to the target fix. When the ATFM system predicts excess demand for an airspace or airport, it assigns a CFDT to an aircraft. In this figure, the time at which the ATFM system determines the CFDT is 8:30. Then, the ATCo instructs the pilot to cross the CFDT fix at the assigned CFDT. The original ETA at the CFDT fix is 9:28, while the CFDT is assigned as 9:30. Therefore, the aircraft must delay the ETA by 2 min. The pilot judges whether the aircraft can comply with the assigned CFDT and replies by either accepting the CFDT or not. The method for complying with the CFDT is determined by the pilot; however, in most cases, the cruise speed is changed.

Such in-flight speed control makes it possible to control the arrival time without extra fuel consumption, whereas arrival time control using vectoring or holding causes higher fuel consumption [6], [7]. Previous studies have investigated the potential benefits of applying in-flight speed control to arrival management or ATFM. Jones et al. developed a speed control algorithm based on integer programming for transferring delay away from the terminal airspace to the en-route phase of flight [8]. Moertl and Pollack presented an airline-based sequencing and spacing system for arrival traffic, including a speed advisory function [9]. Several studies also proposed to combine speed control in the en-route phase of flight with Ground Delay Program, which is a TMI to delay the departure time [10]–[12]. These studies performed simulations with realistic traffic scenarios to illustrate the potential benefits of in-flight speed control for ATFM. Furthermore, Nancy et al. conducted the human-in-the-loop simulation to demonstrate the Integrated Demand Management concept, which combines ATFM and Time-Based Flow Management, including in-flight speed control [13].

B. Operational Environment of CFDT

At present, the CFDT is being considered for application to inbound arrival flights to Tokyo International Airport (RJTT), which is the most congested airport in Japan. Fig. 2 displays the four target routes to which to apply the CFDT, which are referred to as Streams 1 to 4. Note that these routes are different from those in the previous trial operation from 2011 to 2014. The four streams enter the Fukuoka Flight Information Region (Fukuoka FIR) from the west or southwest and enter the Tokyo Approach Control Area (Tokyo ACA) via the SPENS or SELNO waypoint to arrive at RJTT. Table I presents each CFDT stream, CFDT fix, and the distance to the CFDT fix.

The CFDT-determined timing is still under discussion. The candidate timings are when the aircraft flies over the vicinity of FUE, MELEN, TAMAK, and KAZIK/ALBA for each stream, while the CFDT-determined timing is set as the remaining flight time to the entry waypoint to the Tokyo ACA. For example, in Stream 1, the CFDT is determined when the remaining time to SPENS is 80 min; then, the aircraft flies near FUE. To maximize the capability of ATFM, it may be useful to assign an earlier CFDT than the original ETA; however, this study considers only the delay.

C. Problem of CFDT Operation

A critical problem in the previous trial operation of the CFDT was the high rejection rate of the CFDT by the pilot. A high CFDT rejection rate disturbs air traffic and increases the workload for ATCos and pilots. Therefore, it is essential to develop a CFDT procedure with a high acceptance rate to successfully deploy the CFDT operation. One obstacle to achieving a high acceptance rate is that the ATFM system does not know whether the aircraft can comply with the assigned CFDT when calculating the CFDT. The ATFM system, which is a ground system, can access various information related to the target aircraft for the CFDT assignment, such as the route, aircraft type, cruise altitude, cruise speed, and ETA at each waypoint. However, the ATFM system cannot obtain the achievable delay of the target aircraft. If the ATFM system can obtain the achievable delay, it can prevent CFDT

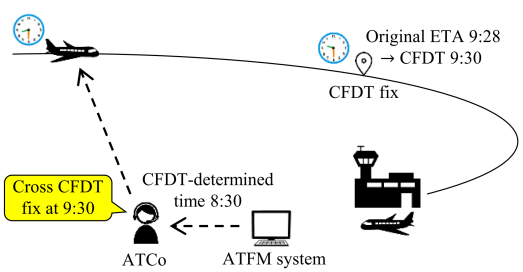

Figure 1: Procedure of the CFDT operation.

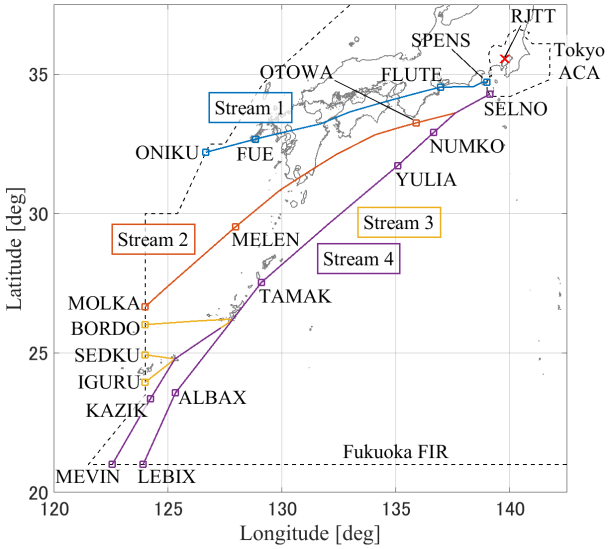

Figure 2: Target routes for CFDT operation.

TABLE I. CFDT streams. Values in parentheses denote distances to the CFDT fix in nautical miles.

Stream	Waypoints	CFDT fix
1	ONIKU–FUE–FLUTE–SPENS (537) (424) (0)	FLUTE
2	MOLKA–MELEN–OTOWA–SELNO (738) (467) (0)	OTOWA
3	BORDO/SEDKU/IGURU–TAMAK–YULIA–NUMKO–SELNO (822) (846) (861) (508) (108) (0)	NUMKO
4	MEVIN/LEBIX–KAZIK/ALBAX–TAMAK–YULIA–NUMKO–SELNO (1047) (994) (879) (616) (508) (108) (0)	NUMKO

rejection by assigning a CFDT within the achievable delay. The achievable delay is highly dependent on the minimum acceptable cruise speed. Note that the minimum acceptable cruise speed is not based only on the aircraft performance, such as the stall speed. In actual operation, the minimum cruise speed is determined by the pilot considering various flight conditions, including the aircraft performance, aircraft mass, and wind conditions. Thus, the minimum acceptable cruise speed differs for each flight. Furthermore, there are several parameters that the ATFM system cannot obtain, such as the deceleration rate of the Mach number. Therefore, the ATFM system cannot obtain the achievable delay.

D. CFDT Operational Model

One method to increase the acceptance rate is to estimate the achievable delay, which can then be used to design the CFDT operation. The CFDT operation model is developed to estimate the achievable delay, and the related parameters are defined in Table II and Fig. 3. Each aircraft is assigned $\Delta CFDT$ calculated by the ATFM system. In addition, each aircraft possesses Δd_{achv} depending on the flight conditions. Then, if $\Delta CFDT$ is equal to or smaller than Δd_{achv}, the pilot accepts the assigned CFDT. In the case presented in Fig. 3, three of four aircraft accept the assigned CFDT; therefore, R_{acpt} is 75 %. $\Delta CFDT_{max}$ is a parameter of the

TABLE II. Parameter definition for CFDT operation.

Symbol	Name	Unit
$\Delta CFDT$	Required delay by the assigned CFDT	[min]
Δd_{achv}	Achievable delay	[min]
R_{acpt}	Acceptance rate	[%]
$\Delta CFDT_{max}$	Maximum assigned CFDT	[min]
Δt_{det}	CFDT-determined timing	[min]

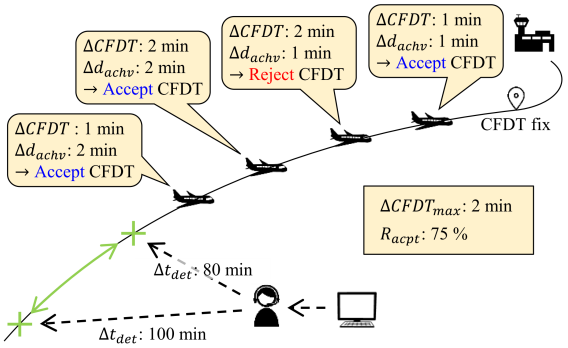

Figure 3: Parameter definition for CFDT operation.

ATFM algorithm, and $\Delta CFDT$ is assigned within $\Delta CFDT_{max}$. To increase the performance of the ATFM, a large $\Delta CFDT_{max}$ is preferable; however, a large $\Delta CFDT_{max}$ might result in a lower R_{acpt}. Therefore, $\Delta CFDT_{max}$ must be set appropriately to achieve a high R_{acpt}. The CFDT is determined Δt_{det} minutes before the original ETA at the CFDT fix. A larger Δt_{det} can produce a larger Δd_{achv}; however, a larger Δt_{det} may cause time prediction errors. Therefore, Δt_{det} must also be set appropriately. $\Delta CFDT_{max}$ and Δt_{det} are the design parameters of the CFDT operation.

Fig. 4 presents the CFDT operational model. The steps of the CFDT operation are as follows:

(1) The aircraft cruises at m_1.
(2) The ATFM system determines $CFDT$ at t_{det}.
(3) The ATCo instructs the CFDT to the pilot.
(4) The pilot judges whether the CFDT is acceptable and controls the aircraft to comply with $CFDT$.
(5) The aircraft decelerates with a_m to and cruises at m_2.
(6) The aircraft flies over the CFDT fix.

Here, $CFDT$ is the assigned CFDT, which can be derived by $ETA_{org} + \Delta CFDT$, where ETA_{org} is the original ETA. m_1 and m_2 are the original cruise and decelerated Mach numbers, respectively. a_m is the deceleration rate of the Mach number. t_{det} is the CFDT-determined time, which can be derived by $ETA_{org} - \Delta t_{det}$. t_1 and t_2 are the start and end times of the deceleration, respectively. Δt_{prcs} is the processing time by the ATCo and pilot. After being assigned the CFDT, the aircraft starts to decelerate to comply with the CFDT. There is a delay from the CFDT-determined time to the start of deceleration due to the processing time by the ATCo and pilot, such as during voice communication. The delay time is defined as Δt_{prcs}. By the deceleration,

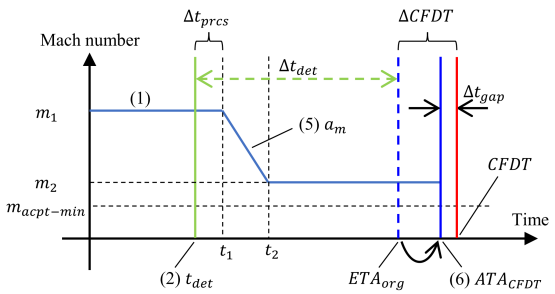

Figure 4: CFDT operational model.

the ETA at the CFDT fix is delayed. The time at which the aircraft flies over the CFDT fix is denoted as the actual time of arrival at the CFDT fix ATA_{CFDT}, and Δt_{gap} is the difference between ATA_{CFDT} and $CFDT$, and is defined as $ATA_{CFDT} - CFDT$. Accordingly, when Δt_{gap} is negative, the aircraft flies over the CFDT fix earlier than $CFDT$, and when it is positive, the aircraft flies over the CFDT fix later than $CFDT$. It is difficult for the aircraft to fly over the CFDT fix at the exact $CFDT$. Thus, if Δt_{gap} is sufficiently small, it is assumed that the aircraft can comply with the assigned CFDT; however, the threshold to comply is still under discussion. $m_{acpt-min}$ denotes the acceptable minimum cruise Mach number. Δd_{achv} is maximized when m_2 is equal to $m_{acpt-min}$. If Δd_{achv} is smaller than $\Delta CFDT$ even with $m_{acpt-min}$, the pilot rejects the assigned CFDT.

Here, if Δt_{prcs}, a_m, and $m_{acpt-min}$ can be derived, Δd_{achv} can be calculated based on the model, as illustrated in Fig. 4. However, the ATFM system cannot directly derive these three parameters; hence, further modeling or data collection is required to calculate Δd_{achv}. Matsuno and Andreeva-Mori developed a model-based estimation method for Δd_{achv} using the Base of Aircraft Data provided by EUROCONTROL and investigated the acceptance rate of the CFDT operation [14]. In contrast, in this study, the approach to estimate Δd_{achv} relies on the analysis of past/current trial data rather than the model-based approach. Namely, the proposed approach can be regarded as a data-driven approach.

III. Operational Trial from 2011 to 2014

A. Collected Data in $SCAS_{2011-2014}$

The trial of the CFDT operation, called the Specifying CFDT for Arrival Spacing Program (SCAS), was conducted from 2011 to 2014. (Hereinafter, the operational trial is denoted as "$\mathrm{SCAS}_{2011-2014}$".) In this period, the routes and airspace configuration were different from those in Fig. 2, but the actual data for performing the CFDT operation were available, such as output data from the ATFM system and radar data. The data from ATFM system included t_{det}, $CFDT$, the CFDT fix, and the callsign and aircraft type of the target aircraft for the CFDT operation. The radar data consisted of the time, latitude, longitude, and pressure altitude. The radar data did not contain the Mach number; however, it could be estimated by synthesizing the time derivative of the position and wind data. The details of the mach number estimation is shown in Appendix A. Figs. 5 and 6 present example results for the cases in which the aircraft could and could not comply with the assigned CFDT, respectively. Here, it was assumed that the aircraft could comply with the assigned CFDT if Δt_{gap} was within $\pm$ 0.5 min. The horizontal axis of the pressure altitude/Mach number is Japan Standard Time. The Mach number oscillates because the Mach number is estimated from the radar data and includes estimation noise. In both cases, the aircraft was assigned a later CFDT than the original ETA at the CFDT fix; therefore, the aircraft reduced the Mach number. In Fig. 5, the aircraft could comply with the assigned CFDT because Δt_{gap} was within $\pm$ 0.5 min. In contrast, Δt_{gap} in Fig. 6 was outside of $\pm$ 0.5 min and negative. This result demonstrates that the aircraft flew over

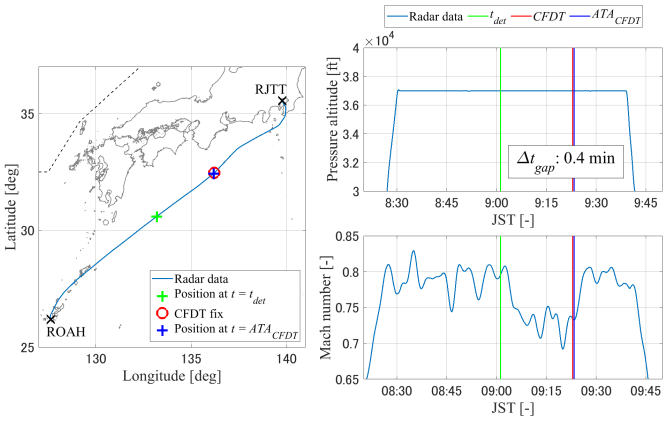

Figure 5: Example from the $\mathrm{SCAS}_{2011-2014}$ trial in the case that the aircraft could comply with the assigned CFDT.

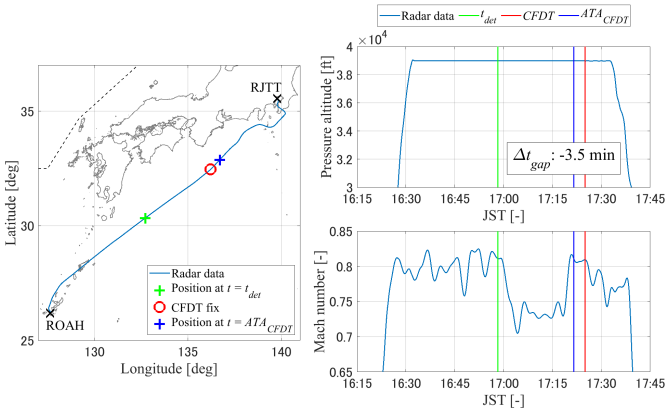

Figure 6: Example from the $\mathrm{SCAS}_{2011-2014}$ trial in the case that the aircraft could not comply with the assigned CFDT.

the CFDT fix earlier than the assigned CFDT and could not comply with the assigned CFDT. It is presumed that the achievable delay was smaller than the required delay even if the aircraft decelerated to the acceptable minimum Mach number. If the CFDT could be assigned appropriately considering Δd_{achv}, the aircraft might be able to comply with the CFDT even in this case.

B. Optimization-Based Mach Number Estimation

The parameters Δt_{prcs} and t_{det} described in II-D could be estimated from the results of $\mathrm{SCAS}_{2011-2014}$. However, the Mach number includes estimation noise. To estimate a clean Mach number, as illustrated in Fig. 4, optimization-based Mach number estimation was performed. The Mach number estimation problem can be formulated as the following optimization problem:

$$\boldsymbol{x} = [t_1 \quad t_2 \quad m_1 \quad m_2]^T, \tag{1}$$

$$\min_{\boldsymbol{x}} \begin{cases} (m(t) - m_1)^2 & \text{if } t_0 \le t < t_1 \\ (m(t) - (a_m t + b_m))^2 & \text{if } t_1 \le t < t_2 \\ (m(t) - m_2)^2 & \text{otherwise} \end{cases}, \tag{2}$$

$$
\begin{aligned}
t_{det} &\leq t_1, \\
t_1 &\leq t_2, \\
t_2 &\leq t_f,
\end{aligned} \tag{3}
$$

where t_{det}, t_1, t_2, m_1, and m_2 correspond to the parameters in Fig. 4. $m(t)$ is the Mach number derived from the radar data. t_0 and t_f are the initial and terminal time of $m(t)$, respectively. In this case, t_0 was set as the entry time to the Fukuoka FIR or the time at the top of climb, and t_f was set as ATA_{CFDT}. In addition, a_m and b_m denote the slope and intercept of the Mach number in the deceleration phase; therefore, these parameters can be derived as follows:

$$
\begin{aligned}
a_m &= \frac{m_2 - m_1}{t_2 - t_1}, \\
b_m &= m_1 - a_m t_1.
\end{aligned} \tag{4}
$$

The formulated optimization problem is a type of nonlinear programming problem and can be solved using the MATLAB® fmincon function.

A clean Mach number can be derived by solving the formulated optimization problem. Fig. 7 and Table III present the optimization results of the flight shown in Fig. 5. The optimization results can estimate a clean Mach number from the Mach number derived by the radar data.

The optimization-based Mach number estimation is performed for all available data, including 153 flights. Fig. 8 presents the distribution of Δt_{prcs} and a_m. Note that not all the flights delayed their arrival as much as possible in actual operation. Several flights could comply with the assigned CFDT without deceleration. As a result, several flights had an excessively large Δt_{prcs}. Table IV presents the average and median of Δt_{prcs} and a_m. Due to the flights without deceleration, the average Δt_{prcs} is more than twice the median Δt_{prcs}. The goal of this analysis is to extract the representative value of Δt_{prcs} and a_m in the case that the aircraft delayed their arrival as much as possible. Accordingly, the median value of Δt_{prcs} and a_m is used to reduce the consequences of an excessively large value.

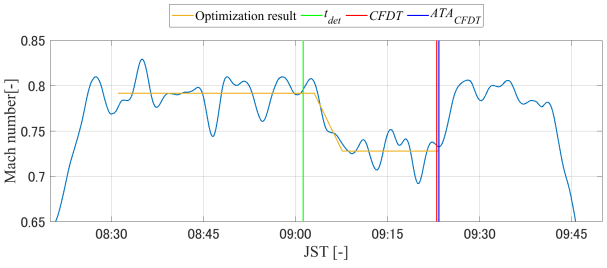

Figure 7: Example results of optimization-based Mach number estimation.

TABLE III. Example results of optimization-based Mach number estimation.

Parameters	Value	Unit
m_1	0.79	[-]
m_2	0.73	[-]
Δt_{prcs}	1.8	[min]
a_m	-0.014	[1/min]

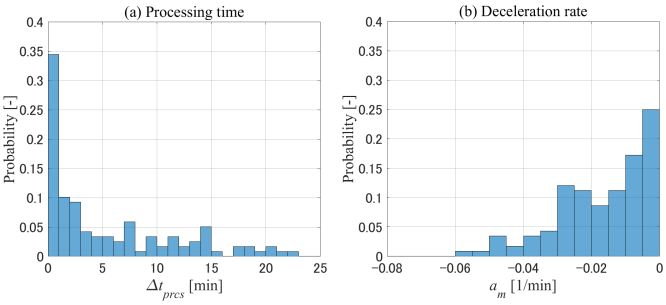

Figure 8: Distribution of the (a) processing time by the ATCo and pilot and the (b) deceleration rate of the Mach number.

TABLE IV. Average and median processing time by the ATCo and pilot (Δt_{prcs}) and the deceleration rate of the Mach number (a_m).

Parameters	Average	Median	Unit
Δt_{prcs}	5.4	2.4	[min]
a_m	-0.017	-0.013	[1/min]

IV. Shadow Operation

A. Collected Data in Shadow Operation

The Shadow Operation was conducted from September to December 2020 and is also planned for 2021 before resuming the CFDT operation. In the Shadow Operation, the aircraft actually did not decelerate, but several data related to the CFDT operation were collected from the onboard system via voice communication. The collected data included the CFDT fix, time at which the ATCo requested the onboard data from the pilot, cruising altitude, cruise Mach number, acceptable maximum/minimum Mach number, and the call-sign and aircraft type of the target aircraft. The collected data were combined with the corresponding radar data to obtain the time history of the position and altitude. The available data were 96 flights in Stream 1, 107 flights in Stream 2, and 194 flights in Stream 3 and 4. As mentioned in II-D, the achievable delay Δd_{achv} can be estimated if Δt_{prcs}, a_m, and $m_{acpt-min}$ are given. The collected data included the acceptable minimum Mach number $m_{acpt-min}$. Therefore, Δd_{achv} could be estimated by applying Δt_{prcs} and a_m derived in III-B to the Shadow Operation data. Furthermore, the acceptance rate of the flights in the Shadow Operation could be estimated using the estimated Δd_{achv}.

B. Simulation-Based Acceptance Rate Estimation

A numerical simulation is used to estimate Δd_{achv}. In the simulation, the flight trajectory is calculated based on integral calculation under the following assumptions:

- The aircraft flew along the CFDT streams.
- The aircraft cruised at cruising altitude, with the cruise Mach number as collected data.
- The time at which the ATCo collected the data was considered the CFDT-determined time t_{det}.

Then, the time history of the Mach number is set based on the CFDT operational model as follows:

- Add Δt_{prcs} to t_{det} to derive the time to start deceleration.

- Decelerate by a_m to $m_{acpt-min}$.
- Cruise at $m_{acpt-min}$ until reaching the CFDT fix.

The details of the trajectory simulation is shown in Appendix B.

Fig. 9 presents an example result of the simulation. In this example, the aircraft flew along Stream 2 whose CFDT fix was OTOWA. The data were collected around MELEN, and $m_{acpt-min}$ was 0.75. On the right side of Fig. 9, the Mach number is plotted from the time of data collection, which is assumed as t_{det}. Here, "Without deceleration" denotes the case in which the aircraft continues to cruise at the cruise Mach number to derive the original ETA, while "With deceleration" denotes the case in which the aircraft decelerates to $m_{acpt-min}$ to delay its arrival as much as possible. After Δt_{prcs}, the aircraft decelerates by a_m to $m_{acpt-min}$. In the case without deceleration, ATA_{CFDT} is 17:42:20, while ATA_{CFDT} with deceleration was 17:44:31. As a result, Δd_{achv} can be estimated as 2.2 min in this flight.

Fig. 10 presents the simulation results for all the flights. Each cumulative distribution function (CDF) denotes Δd_{achv} in each stream. Here, Stream 1 is 0.44 at 1 min, signifying that the remaining 56 % of flights can comply with a delay of 1 min or more; namely, the acceptance rate R_{acpt} is equal to 56 % in Stream 1 when $\Delta CFDT_{max}$ = 1. In fact, Fig. 10 presents the compliance rate, which expresses how many flights are able to comply with the assigned CFDT. There is a small possibility that the pilot accepts the CFDT if the aircraft cannot comply with the assigned CFDT, and similarly, that the pilot does not accept the CFDT even if the aircraft can comply with it. However, in this analysis, it is assumed that the compliance rate is equivalent to R_{acpt}. Stream 3/4 (TAMAK) represents the result in Streams 3 and 4 in the case

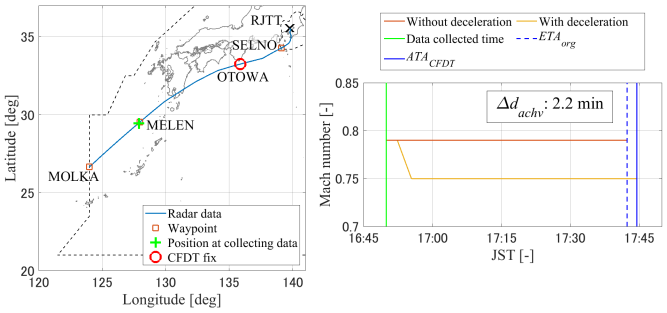

Figure 9: Example results of the achievable delay estimation.

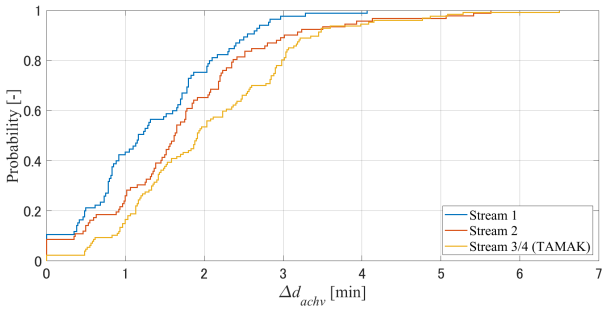

Figure 10: CDF of the achievable delay in each stream.

that the data were collected near TAMAK. Table V presents the estimated R_{acpt} in each stream with different $\Delta CFDT_{max}$. In all the streams, R_{acpt} was higher with a shorter $\Delta CFDT_{max}$. Stream 3/4 (TAMAK) had the highest R_{acpt} among the three streams because it had the largest Δt_{det}.

V. Discussion

In the optimization-based Mach number estimation discussed in III, Δt_{prcs} and a_m can be estimated from the $\mathrm{SCAS}_{2011-2014}$ data. This method is a post-analysis method because the estimation is applied to the radar data used for the CFDT operation. The available data of $\mathrm{SCAS}_{2011-2014}$ are limited and differ from the current operational environment, but the same method can also be applied to the radar data derived from future CFDT operation. A large amount of data can make it possible to estimate Δt_{prcs} and a_m more accurately.

In the simulation-based acceptance rate estimation discussed in IV, Δd_{achv} can be calculated using the Shadow Operation data and Δt_{prcs} and a_m derived by the optimization-based Mach number estimation. Finally, R_{acpt} can be estimated from the CDF of Δd_{achv}. The estimation method for the CFDT acceptance rate is useful for designing a CFDT procedure with a high acceptance rate. In Table V, with $\Delta CFDT_{max}$ = 1 and 2, R_{acpt} in Stream 3/4 (TAMAK) is 83 % and 46 %, respectively. Therefore, it is presumed that $\Delta CFDT_{max}$ should be set to 1 for Stream 3/4 (TAMAK). However, if it is desirable to set a larger $\Delta CFDT_{max}$ from the viewpoint of the ATFM operation, one option is to set a longer CFDT-determined timing. For example, in the Shadow Operation, the flights in Stream 4 were collected data near KAZIK/ALBAX in addition to TAMAK. Fig. 11 and Table VI present the results of the acceptance rate estimation in Stream 4 with different CFDT-determined timings. The results indicate that R_{acpt} in Stream 4 (KAZIK/ALBAX) is higher than that in Stream 4 (TAMAK). Determining $CFDT$ far away from the CFDT fix may increase the trajectory estimation error; however, $\Delta CFDT_{max}$ can be increased to

TABLE V. CFDT acceptance rate in each stream.

$\Delta CFDT_{max}$	1 [min]	2 [min]	3 [min]
Stream 1	56 [%]	25 [%]	2 [%]
Stream 2	74 [%]	35 [%]	11 [%]
Stream 3/4 (TAMAK)	83 [%]	46 [%]	20 [%]

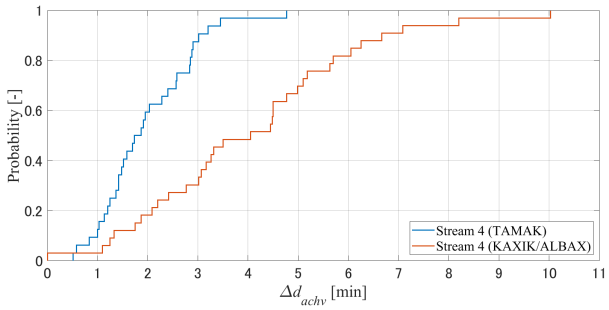

Figure 11: CDF of the achievable delay in Stream 4.

TABLE VI. CFDT acceptance rate in Stream 4.

$\Delta CFDT_{max}$	1 [min]	2 [min]	3 [min]
Stream 4 (TAMAK)	91 [%]	41 [%]	12 [%]
Stream 4 (KAZIK/ALBAX)	97 [%]	82 [%]	70 [%]

2–3 minutes by setting the CFDT-determined time around KAZIK/ALBAX.

In summary, the proposed analysis method can contribute to the design of an efficient CFDT operational procedure by providing the estimated acceptance rate. Furthermore, with a database containing sufficient parameters to estimate the acceptance rate, such as Δt_{prcs}, a_m, and $m_{acpt-min}$, the ATFM system can calculate Δd_{achv} in real time and dynamically assign Δd_{achv} to each flight. This CFDT operation has the potential to improve the performance of the ATFM operation.

VI. Conclusion

This paper proposes data-driven analysis methods for the CFDT operation, which is an in-flight speed control TMI. The analysis methods include an optimization-based method for Mach number estimation and a simulation-based method for estimating the CFDT acceptance rate. Both methods were investigated using actual data derived in $\mathrm{SCAS}_{2011-2014}$ and the Shadow Operation. The acceptance rate of the CFDT assignment was calculated, and the applications were discussed. The results indicate that the maximum assigned CFDT can be increased to 2–3 min by changing the CFDT-determined time.

Future work will include a stochastic analysis of the potential benefit from the CFDT assignment. The next Shadow Operation is planned for late 2021. With additional data, the CFDT acceptance rate will be modeled. The model of the CFDT acceptance rate will be applied to the combined air traffic simulator, which is composed of the ATFM and terminal traffic simulators [17]. The combined air traffic simulator can evaluate the stochastic performance of the ATFM. The potential benefit from the CFDT assignment will be estimated stochastically by comparing the ATFM with and without the CFDT assignment in the simulator.

Acknowledgment

We would like to express our sincere thanks to the Japan Civil Aviation Bureau for providing the radar, ATFM, and Shadow Operation data.

Appendix A. Mach number estimation

The Mach number is estimated from the radar and wind data as following steps:

- The geodetic length and azimuth angle of the trajectory are calculated from the latitude and longitude by using the inverse calculation [15].
- The ground speed (GS) is derived from the time derivative of the geodetic length.
- The true airspeed (TAS) is estimated by synthesizing the GS with wind data according to Eq. (5).

$$v_{tas} = \sqrt{(v_{gs} - w_a)^2 + w_c^2}, \tag{5}$$

where v_{tas} is the TAS, v_{gs} is the GS, w_a is the along-track wind speed, and w_c is the cross-track wind speed, respectively. The geometry of the GS, TAS, and wind speed are shown in Fig. 12, where w_n and w_e are the meridional and zonal winds. The wind data is derived from the numerical weather prediction (NWP) data based on the meso-scale model (MSM) provided by the Japan Meteorological Agency [16].

- m is calculated from v_{tas} by using Eq. (6).

$$m = \frac{v_{tas}}{\sqrt{\kappa R T}}, \tag{6}$$

where κ is the heat capacity ratio for air, and R is the real gas constant for air. T is the atmospheric temperature which also can be derived from the NWP MSM data.

Appendix B. Trajectory simulation

The flowchart of the trajectory simulation is shown in Fig. 13. The position when $t = t_{det}$ is set as the initial posi-

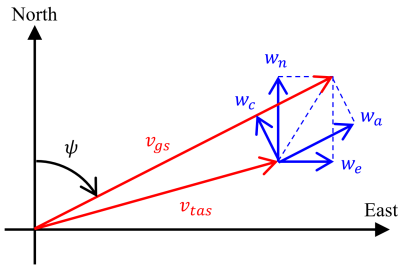

Figure 12: Geometry of GS, TAS, and wind speed.

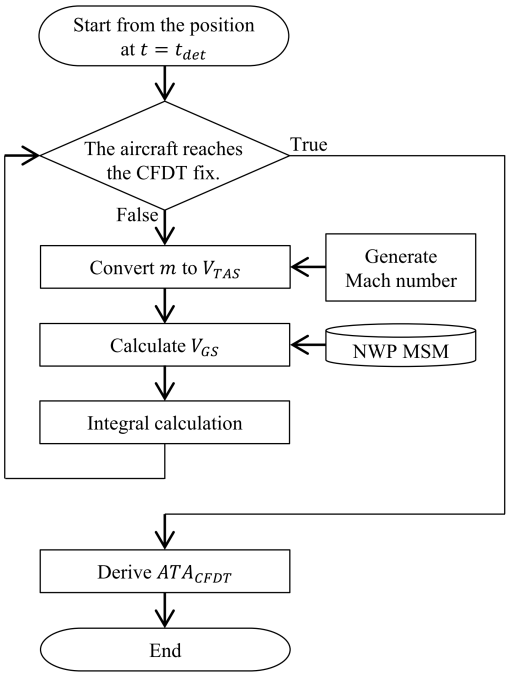

Figure 13: Flowchart of the trajectory simulation.

tion of the trajectory simulation. The trajectory is calculated by the time integral of v_{gs} from the initial position to the CFDT fix. m is generated from the time history of the Mach number described in IV-B and converted to v_{tas} according to Eq. (7).

$$v_{tas} = m\sqrt{\kappa RT}. \tag{7}$$

v_{gs} is calculated by synthesizing v_{tas} and NWP MSM wind data, as follows:

$$v_{gs} = \sqrt{(v_{tas} - w_c)^2 + w_a^2}. \tag{8}$$

The trajectory simulation is terminated when the aircraft reaches the CFDT fix. Then, ATA_{CFDT} can be derived.

REFERENCES

[1] Japan Civil Aviation Bureau (JCAB), "Air traffic flow management (ATFM)," https://www.mlit.go.jp/common/001132169.pdf (accessed March, 2021)

[2] Federal Aviation Administration (FAA), "Traffic management initiatives," Air Traffic Plans and Publications, Order 7210.3BB, Part 5, Chapter 18, Section 6, https://www.faa.gov/air_traffic/publications/atpubs/foa_html/chap18_section_6.html (accessed March, 2021)

[3] Japan Civil Aviation Bureau (JCAB), "ATFM/CDM in JAPAN," The Third Meeting of Air Traffic Flow Management Steering Group, PPT02, 2014.

[4] New Zealand and Singapore, "Long range ATFM concept trials," Eighth Meeting of the Asia/Pacific Air Traffic Flow Management Steering Group (ATFM/SG/8), IP/06, 2018.

[5] Japan Civil Aviation Bureau (JCAB), Japan Aeronautical Information Service Center (AIS JAPAN), "Operational trial for specifying calculated fix departure time (SCAS) for air traffic flow management," Aeronautical Information Circular, Nr 029/11, 28 JUL 2011, 2011.

[6] X. Prats and M. Hansen, "Green delay programs, absorbing ATFM delay by flying at minimum fuel speed," 9th USA/Europe Air Traffic Management Research and Development Seminar (ATM Seminar), Berlin, 2011.

[7] Y. Xu, R. Dalmau, and X. Prats, "Effects of speed reduction in climb, cruise and descent phases to generate linear holding at no extra fuel cost," 7th International Conference on Research in Air Transportation (ICRAT), Philadelphia, 2016.

[8] J. C. Jones, D. J. Lovell, and M. O. Ball, "En route speed control methods for transferring terminal delay," 10th USA/Europe Air Traffic Management Research and Development Seminar (ATM Seminar), Chicago, 2013.

[9] P. M. Moertl and M. E. Pollack, "Airline based en route sequencing and spacing field test results, Observations and lessons learned for interval management," 9th USA/Europe Air Traffic Management Research and Development Seminar (ATM Seminar), Berlin, 2011.

[10] L. Delgado and X. Prats, "Effect of radii of exemption on ground delay programs with operating cost based cruise speed reduction, case study: Chicago O'Hare International Airport," 10th USA/Europe Air Traffic Management Research and Development Seminar (ATM Seminar), Chicago, 2013.

[11] J. C. Jones, D. J. Lovell, and M. O. Ball, "Combining control by CTA and dynamic enroute speed adjustment to improve ground delay program performance," 11th USA/Europe Air Traffic Management Research and Development Seminar (ATM Seminar), Lisbon, 2015.

[12] Y. Xu and X. Prats, "Including linear holding in air traffic flow management for flexible delay handling," 12th USA/Europe Air Traffic Management Research and Development Seminar (ATM Seminar), Seattle, 2017.

[13] N. M. Smith et al., "Integrated demand management: coordinating strategic and tactical flow scheduling operations," AIAA AVIATION Forum, 16th ATIO Conference, Washington, D.C., 2016.

[14] Y. Matsuno and A. Andreeva-Mori, "Analysis of achievable airborne delay and compliance rate by speed control: A case study of international arrivals at Tokyo International Airport," IEEE Access, vol. 8, pp. 90686–90697, 2020.

[15] B. R. Bowring, "Total inverse solutions for the geodesic and great elliptic,". Survey Review, vol. 33, Issue 261, pp. 461–476, 1996.

[16] Japan Meteorological Agency (JMA), JMA numerical weather prediction, https://www.jma.go.jp/jma/jma-eng/jma-center/nwp/nwp-top.htm (accessed April 2021)

[17] D. Toratani, N. Takeichi, and M. Oka, "Simulation study on the interoperability between air traffic flow management and tactical arrival management," ENRI International Workshop on ATM/CNS (EIWAC), Tokyo, 2019.